TDR 2006

Purdue University

Soil Moisture Probes for a Dispersive Soil

S. D. Logsdon and B. K. Hornbuckle

Ref.: Hornbuckle, B. K. and Logsdon, S. D., "Soil Moisture Probes for a Dispersive Soil", Proc. TDR 2006, Purdue University, West Lafayette, USA, Sept. 2006, Paper ID 13, 14 p., https://engineering.purdue.edu/TDR/Papers

Soil Moisture Probes for a Dispersive Soil

S.D. Logsdon[1] and B.K. Hornbuckle[2]

[1]Soil Scientist, USDA-ARS, NSTL, 2150 Ames, IA 50011; PH (515)294-8265; email: logsdon@nstl.gov

[2]Assistant Professor, Iowa State University, Ames, IA 50011; PH (515)294-9868; email: bkh@iastate.edu

Abstract

Soils high in smectite clays have presented difficulties when using dielectric soil moisture sensors in the field. The purpose of this study was to determine which soil moisture sensor provided reliable data on these soils after site-specific calibration. The CS616[1] water content reflectometer was compared in the field and laboratory with the ML2X[2] theta probe and the Hydra[3] probe. The soil was Canisteo clay loam (Fine-loamy, mixed, superactive, calcareous, mesic Typic Endoaquoll). The CS616 was installed horizontally in the field at 1.5 and 4.5 cm depths (one each depth), and the ML2X and Hydra probes were installed horizontally centered at 3 cm depth (four each probe). Gravimetric soil moisture samples were taken on five dates. Then all the probes were installed in repacked soil columns or cores for laboratory analysis. Additional measurements were made with a twelve wire probe using a vector network analyzer (VNA) in similar packed cores. Data from the CS616 was theoretically converted to apparent permittivity, and data from the ML2X was empirically converted to apparent permittivity using the manufacturer's equation. The Hydra probe program estimates real and imaginary parts of permittivity. The measurement volume was larger for the CS616 than for the other probes because of the longer electrodes and because of the two-electrode (parallel) configuration. This provided greater consistency between the measurements for CS616. However, the larger volume may have allowed some energy to extend beyond the soil surface for the shallow probe in the field. The permittivity values correlated with water content and among probes, but the values were not identical among probes or with that determined from vector network analyzer. Temperature correction improved field soil water patterns. Lower cost and larger measurement volume favored the CS616 over the other probes.

Key words: dielectric sensors, permittivity, soil water content, measurement volume

[1] Campbell Scientific, Inc., Logan, Utah
[2] Stevens Vitel, Inc., Cantilly, Virginia
[3] Delta-T Devices, Inc., Cambridge, UK

Mention of specific equipment is for information only and does not constitute endorsement by the USDA.

Introduction

Understanding the water balance in the field is complicated because water moves laterally in the subsurface (Anderson and Burt, 1990[2]; Philip, 1991[16]; Jackson, 1992[4]) as well as vertically both down to the water table and up from a shallow water table in response to gradients created by root water extraction and evaporation (Van Bavel et al., 1968[19]; Allmaras et al., 1975[1]; and Van Bavel and Ahmed, 1976[20]; Maroux and Lafolie, 1998[13]). Recent techniques have been developed to quantify the lateral water movement and upward water movement (Morgan and Stolt, 2004[14]; Nachabe et al., 2005[15]), but these techniques require automated soil water content measurements. Traditional time domain reflectometer (TDR) has been used for automated determination of soil water content, but hardware limitations present difficulties. This is a serious problem for soils high in smectite clay (Logsdon, 2000[9], 2005b[11], 2006[12]), especially for multiple sites, which required multiplexers and long coaxial cables. The problem is complicated waveform analysis for problem soils. Computer programs can handle these difficult waveforms, but internal data logger programs cannot. Saving or analyzing automated waveform data has large data storage requirements that require electricity to run a computer in the field. Since electricity is rarely available, a data logger is used that can run off a marine battery / solar panel, but can only save the single calculated value, not the whole waveform.

The purpose of this study is to verify the accuracy of selected automated soil moisture sensors for soils high in smectite clays, and to compare with dielectric spectra results. This is a preliminary study that will help us determine the type of sensor to use in future field experiments. A much more comprehensive study will be made over the next several years as part of a larger effort to continuously measure all aspects of terrestrial water cycle (precipitation, soil water storage, drainage, runoff, and evapotranspiration) over the entire year in an agricultural field near Ames, IA. The preliminary study is restricted to a soil similar to that in the planned field experiment, since site-specific calibration would be needed for other soils not in the planed site.

Materials and Methods

Field sensor placement

We installed soil moisture sensors horizontally in the field on Canisteo silty clay loam The sensors installed included the CS616, ML2X, and Hydra probes. One CS616 was installed each at 1.5 and 4.5 cm depths, and four each of Hydra and ML2X were installed at 3.0 cm depth. The sensors were spaced apart as was practical within the ranges of cables; all sensors were located within a 20 m X 20 m area. After all the equipment was working, soil samples were taken for gravimetric water content and bulk density by pushing 3.8 cm long and 7.4 cm diameter cores into the soil at two depths. Much of the data early in the season was not usable because one solar panel was not enough; another solar panel was added in July. After this date we collected gravimetric samples on five dates for 0-3.8 cm and 4-7.8 cm. Data were interpolated between these depths. We were not able to enter the field immediately after rain events, so only dry and medium soil water contents were included. Because the Hydra probe had temperature measurements in the head, a temperature-corrected field calibration was done for this probe.

Background Sensor Information

The measurement frequency varied among the different sensors. The frequency bandwidth for the CS616 is 175 MHz (Kelleners et al., 2005b[7]), and the data would tend to be at the upper end of the range. The ML2X probe operates at a frequency of 100 MHz (Delta-T Devices, 1999[3]), and the Hydra probe operates at a measurement frequency of 50 MHz (Steven-Vitel, 1994[18]).

For comparison, the ML2X voltage was converted to the square root the apparent permittivity, $\varepsilon_a^{1/2}$, using the empirical equation from the company (Delta-T Devices, 1999[3]):

$$\varepsilon_a^{1/2} = 1.07 + 6.4V - 6.4V^2 + 4.7V^3 \tag{1}$$

where V is the measured voltage. For the Hydra probe the company program converts three of the voltage outputs to estimates of the real and imaginary components of permittivity (Steven-Vitel, 1994[18]); for this study, the square root of the real permittivity ($\varepsilon'^{1/2}$) was used for calibration and $\varepsilon_a^{1/2}$ for comparisons among probes. The CS616 output was converted to square root of apparent permittivity as described by Kelleners et al. (2005b[7]):

$$\varepsilon_a^{1/2} = \frac{(t - 2t_d)c}{4L} \tag{2}$$

where $L \sim 26$ cm (probe length), $t_d \sim 5.4 \times 10^{-9}$ s, c is speed of light (3.0×10^8 m s^{-1}), $t = P/S_t$, S_t = 1024, and P is the period instrument output (s). Figure 1 shows the relative size of the sensors.

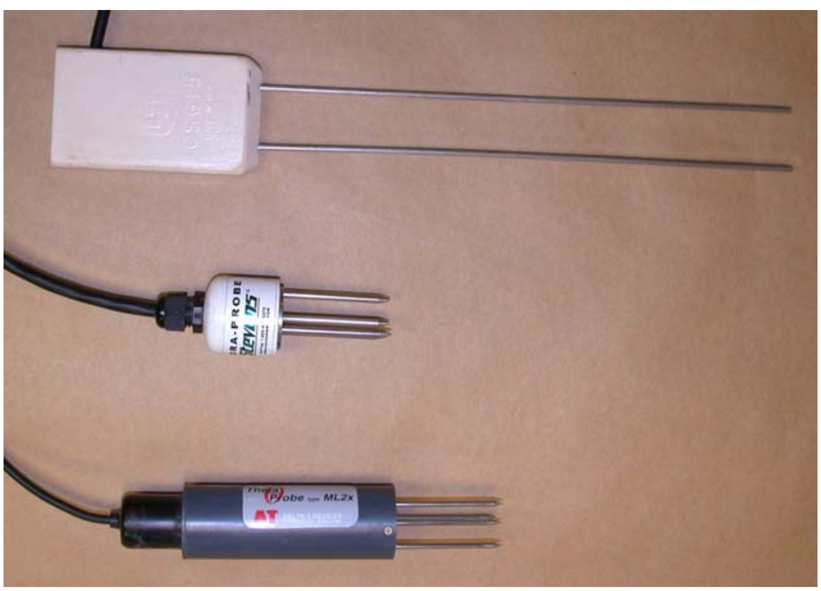

Fig. 1. The CS616 (top) , Hydra (middle), and ML2X (bottom) probes used in this study.

Laboratory calibration

Before harvest, the equipment was removed, and after harvest bulk soil was collected from surface soil at the site. This soil was packed into stainless steel cylinders 7.4 cm diameter and 7.6 cm long, as well as acrylic columns 6.8 cm diameter and 33 cm long. We attempted to pack to 1.3 g cm^{-3}, but actual density ranged from 1.0 to 1.3 g cm^{-3}. Each sample was adjusted to a range of water contents and two temperatures. For the CS616 and ML2X the laboratory calibration equations included soil water as a function of temperature and $\varepsilon_a^{1/2}$. These equations were specifically appropriate for the laboratory samples. The field calibrations were determined without temperature correction. Then they were redetermined using the temperature coefficient from the laboratory data. For the Hydra probe, the field temperatures for each probe were used to determine the field temperature coefficient. Calibration equations were determined through fitting by least squares regression.

The calculated water contents using the calibration equations were compared with the measured water contents. For each probe, root mean square error (RMSE) was compared for calibrations with and without temperature correction

$$RMSE = \frac{\sum vd^{2}}{n} \qquad (3)$$

where *vd* is the difference between predicted and measured water contents and *n* is the number of samples. Coefficients of variation (CV) were determined for gravimetric water contents on each field measurement date, as well as for the variability of the different sensor types.

We collected from the Agilent 8753E vector network analyzer (VNA) to examine the variation with frequency. We developed a prototype twelve wire probe, six inner and six outer, approximate coaxial. The twelve wires for our probe were originally 5.0 cm long cylinders, connected to the BNC connector within a 0.9 cm thick epoxy head. Only 4.7 cm of wire extended beyond the head. The wire diameter was 1 mm, the spacing of the inner six wires was 1.7 cm, and the spacing for the outer six wires was 5.1 cm. The electrical length of the twelve wire probe was determined using the same fluids and procedure as used for the truncated coaxial cell (Logsdon, 2005a[10]). The determined electrical length was 0.1236 m and the impedance was 193 ohms.

In preparation for the twelve wire test, soil was packed into steel cylinders 7.4 cm diameter and 7.6 cm long. The twelve wire probe was placed on the surface of the soil and gently inserted. The samples were adjusted to a range of water contents. Permittivity spectra were determined as described by Logsdon (2005a[10]). The square root of the apparent permittivity was determined from the quarter wavelength procedure at the resonance frequency, f_R:

$$\varepsilon_a^{1/2} = \frac{c}{4Lf_R} \qquad (4)$$

where L is the electrical length of the sample and f_R is the longitudinal resonance frequency (Heimovaara et al., 1996[5]; Shang et al., 1999[17]; Logsdon, 2005a[10]).

Energy distribution

One consideration is the energy distribution. Knight (1992[8]) showed for a coaxial system that

$$\frac{r_m}{r_2} = (\frac{r_1}{r_2})^{1/2} \qquad (5)$$

where r_m is the median energy radius (equivalent to 50% of the energy if no attenuation), and 1 and 2 subscripts refer to inner and outer radii of the coaxial cell. The equation for a parallel probe would be

$$J = \frac{\ln(f/b)}{\ln(d/b)} \qquad (6)$$

where d is the half distance between the center of the two wires, b is the radius of each wire, and f is the outer distance for half of the energy when J is set to 0.5.

Results and Discussion

Variability of Field Data

The mean soil water content for the five sampling dates ranged from 0.139 to 0.267 $m^3\ m^{-3}$ for the 1.5 cm depth with CVs from 7-13%, ranged from 0.161 to 0.272 $m^3\ m^{-3}$ for the 3 cm depth with CVs from 7-12%, and ranged from 0.204 to 0.314 $m^3\ m^{-3}$ for the 4.5 cm depth wtih CVs from 5-11%. The CVs for the four ML2X probes for these sampling times ranged from 3-4%, and for the four Hydra probes ranged from 7-13%. Natural site-to-site variation would be expected.

Field and Laboratory Calibration

Permittivity spectra from VNA (Figure 2) are unexciting because of limited useful frequency range. The $\varepsilon_a^{1/2}$ spectra from VNA data increased at lower frequencies (Figure 2) due to electrical conductivity contribution to the imaginary component as well as relaxation contributions. Both contributions are indicated in Equation 7

$$\varepsilon''(f) = \frac{\sigma_{dc}}{2\pi f \varepsilon_v} + \varepsilon_R'' \qquad (7)$$

where ε'' is the imaginary component, f is frequency, σ_{dc} is the direct current electrical conductivity, ε_v is the permittivity of a vacuum (8.854 X 10^{-12} F m^{-1}), and ε_R'' is the relaxation component of imaginary permittivity. The $\varepsilon_a^{1/2}$ is derived from both real and imaginary components of permittivity:

$$\varepsilon_a^{1/2} = (\{1 + [1 + (\frac{\varepsilon''}{\varepsilon'})^2]^{1/2}\}\frac{\varepsilon'}{2})^{1/2} \quad (8)$$

where ε' is the real component of permittivity. The $\varepsilon_a^{1/2}$ is the real part of the index of refraction. At low frequencies there was greater spread of $\varepsilon_a^{1/2}$ for low water contents than for high water contents. The highest frequency point in the displayed spectra was calculated at the resonance frequency; the resonance frequency decreased as water content increased (Equation 4).

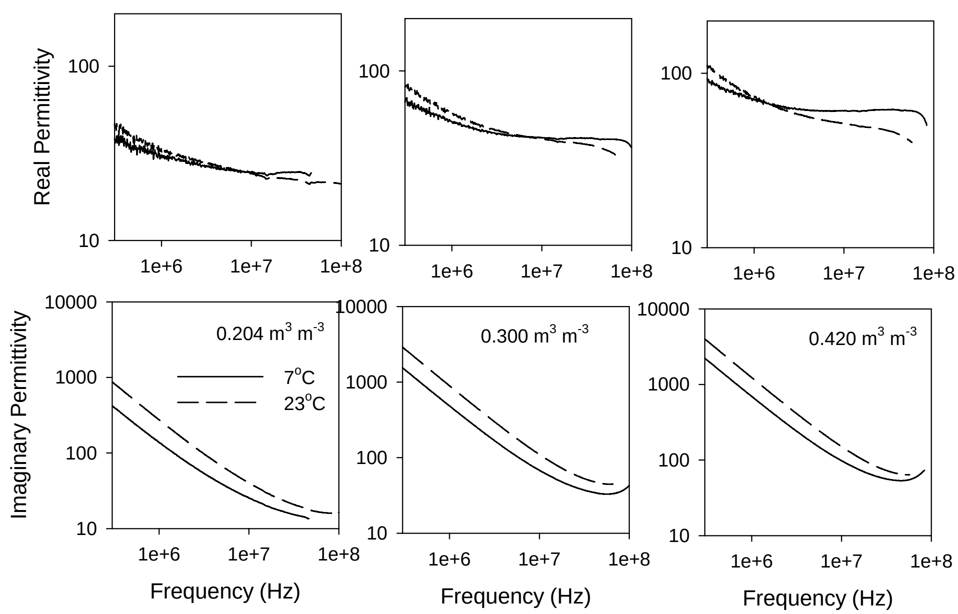

Fig. 2. Real and imaginary permittivity spectra at two temperatures and three water contents.

The increase of $\varepsilon_a^{1/2}$ as frequency decreased (Figure 3) would be expected to result in different $\varepsilon_a^{1/2}$ values for different probes because of the varied measurement frequency. Comparing laboratory calibration data for all probes (Figure 4, Table 1) showed that at any given water content, the ML2X had the smallest $\varepsilon_a^{1/2}$ and the Hydra probe usually had the largest. Since the Hydra probe operated at the lowest frequency among the probes tested, it was expected to have the largest $\varepsilon_a^{1/2}$. The ML2X gave lower $\varepsilon_a^{1/2}$ partly because an empirical equation rather than a theoretical equation was used for the calculation of $\varepsilon_a^{1/2}$. The empirical factory equation was likely based on expected results for standards at higher frequency. Note that the low slope for VNA was related to the decrease in f_R as water content, hence $\varepsilon_a^{1/2}$, increases (Equation 4). Each probe would need to be specifically calibration on-site for these soils high in smectite clays; therefore the calibration equations (Table 1) were specific for this site.

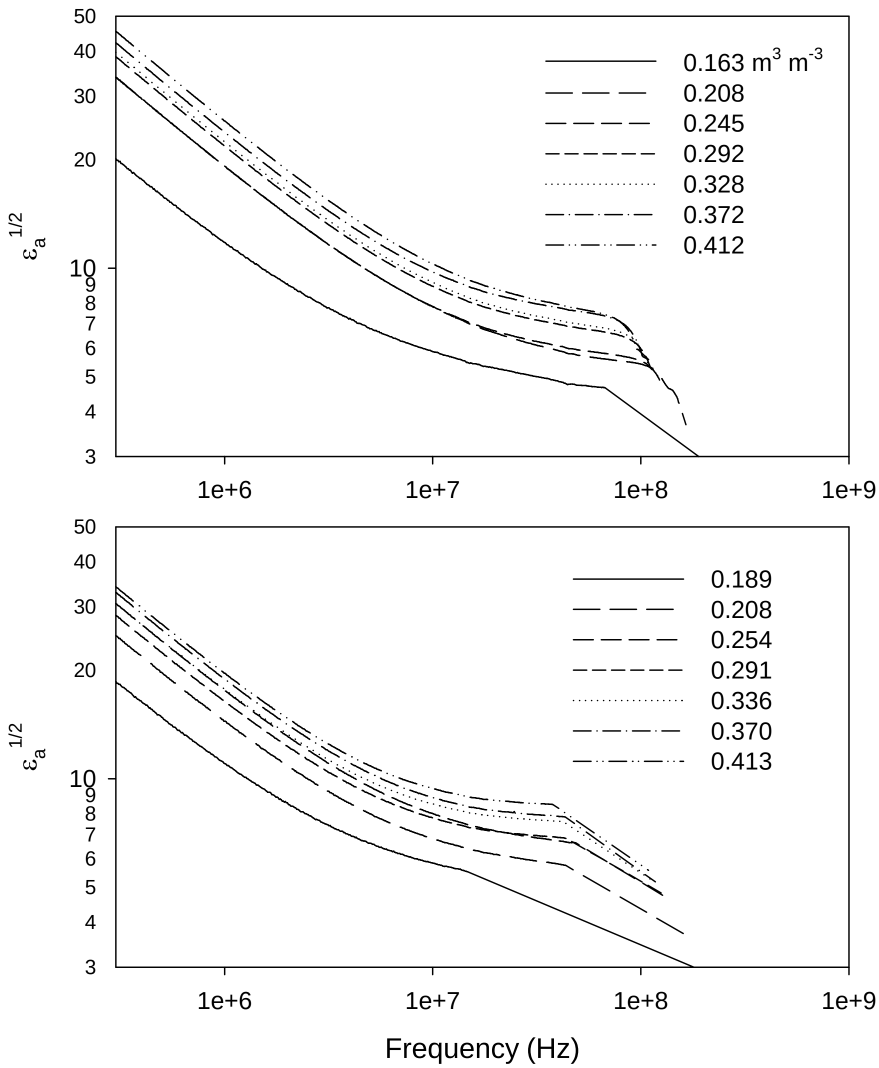

Figure. 3. Square root of apparent permittivity spectra from the vector network analyzer for a sample at approximately 23ºC (upper) and refrigerated to approximately 7ºC (lower).

Table 1. Laboratory and field calibration equations for the different sensors, excluding low water content, and root mean square error between calculated and measured field water contents.

Sensor	Site	Equation	RMSE
VNA	Lab	$\theta = 0.2045* \varepsilon_a^{1/2} - 0.684 - .00259T$	--
ML2X	Lab/field	$\theta = -0.284 + 0.159\varepsilon_a^{1/2} -0.00114T$	$5.5X10^{-4}$
ML2X	Field	$\theta = -0.306 + 0.158\varepsilon_a^{1/2}$	$5.5X10^{-4}$
Hydra	Field	$\theta = -0.002 + 0.0608\varepsilon'^{1/2}$	$1.17X10^{-3}$
Hydra	Field	$\theta = -0.005 + 0.0610\varepsilon'^{1/2} -0.00037T$	$1.30X10^{-3}$
CS616	Lab/field	$\theta = -0.269 + 0.124\varepsilon_a^{1/2} -0.00217T$	$7.0X10^{-4}$
CS616	Field	$\theta = -0.316 + 0.123\varepsilon_a^{1/2}$	$7.0X10^{-4}$

θ is water content, *T* is temperature in Celsius, $\varepsilon_a^{1/2}$ is the square root of the apparent permittivity, $\varepsilon'^{1/2}$ is the square root of the real permittivity, and RMSE is root mean square error.

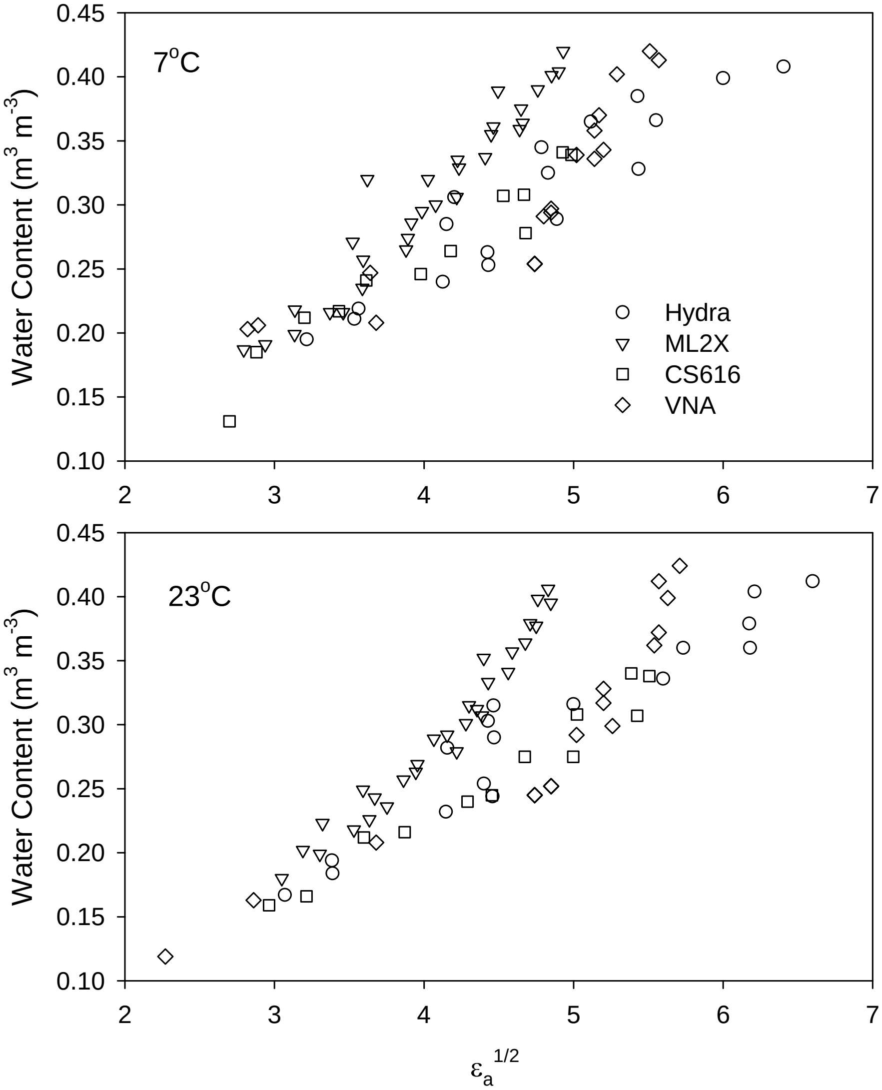

Fig. 4. Calibration comparison for the different sensors.

Calculated water contents for the ML2X showed diurnal fluctuations without the temperature corrections (Figure 5). The temperature from the Hydra probe could indicate a lag within the head; nevertheless, the temperature-corrected data appeared more appropriate for nighttime water contents (level or slanting instead of dipping).

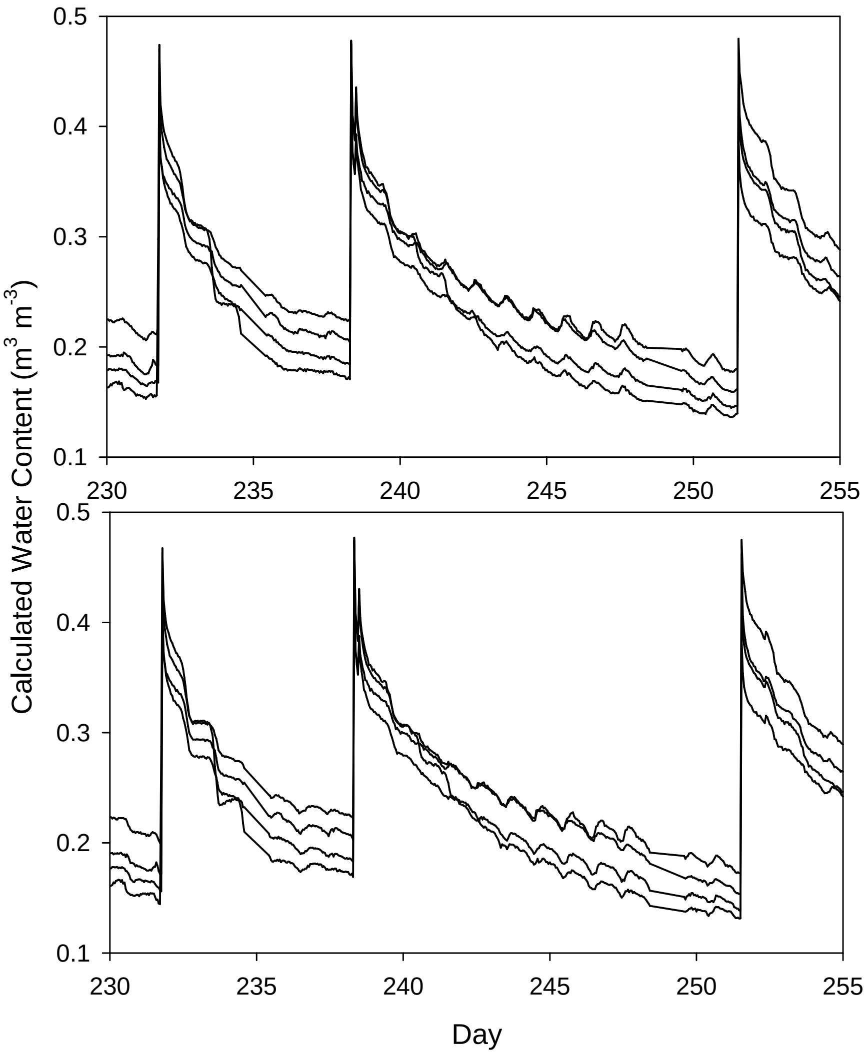

Fig. 5. Theta probe (ML2X) calculated water contents for 3 cm depth based on field calibration with no temperature correction (top) or laboratory / field calibration that included temperature. The lines represent the different sensors.

Some sensor variability and field temperature sensitivity were observed for the Hydra probe (Figure 6) even though temperature effects were not significant from the laboratory calibration.

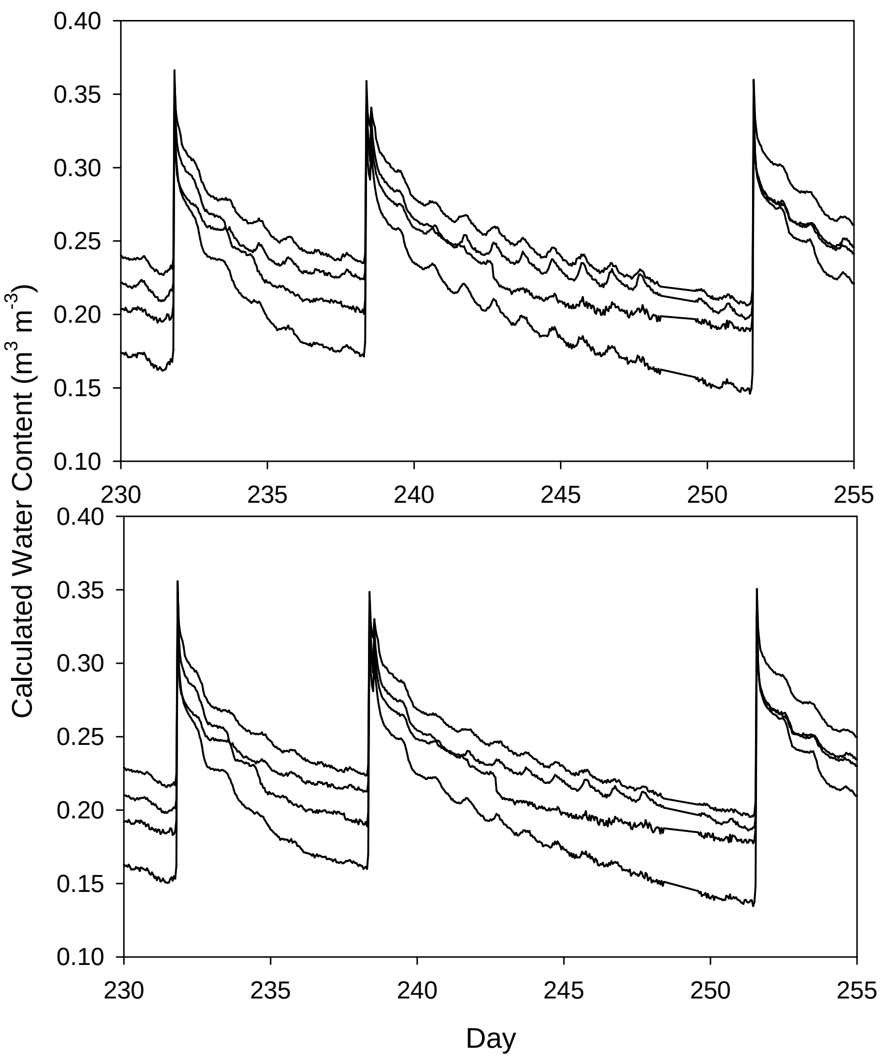

Fig. 6. Hydra probe calculated water contents for 3 cm depth based on field calibration without temperature correction (top), and with temperature correction (bottom). The lines represent different sensors.

For the CS616 the temperature corrected data appeared better for nighttime (Figure 7), again with the temperature lag within the Hydra probe head. Perhaps the higher frequency range resulted in a more uniform response across water contents.

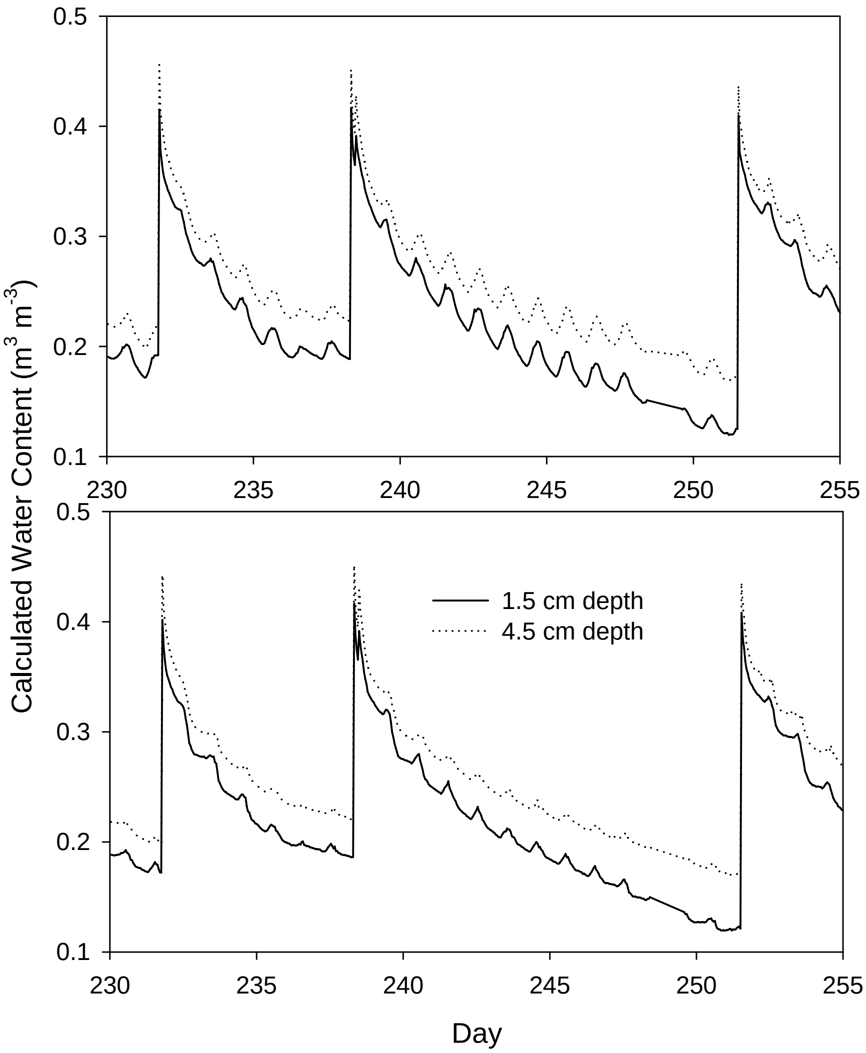

Fig. 7. CS616 calculated water contents for 1.5 and 4.5 cm depths based on field calibration without including temperature (top), and laboratory calibration including temperature (bottom).

Energy Distribution

The energy distribution calculation (Equation 5) for the ML2X showed that 50% of the energy was contained within a 2.8 cm radius of the center wire. The 50% energy measurement volume for the 6 cm long wires would be 148 cm^3. The energy distribution calculation for the Hydra probe showed that 50% of the energy was contained within a 3.0 cm radius of the center wire. The 50% measurement volume for the 5.7 cm long wires would be 161 cm^3. The energy distribution calculation (Equation 6) for the CS616 showed that 50% of the energy was contained within a 1.3 cm radius of each waveguide. The 50% measurement volume for the 30 cm long wires would be 338 cm^3. The energy distribution for the twelve wire probe showed that 50% of the energy extended to 1.5 cm outside the inner six wires, which were spaced 1.7 cm apart. The combined radius is 2.35 cm, less than the radius of the soil cylinder (3.7 cm). Since the length was 4.7 cm, the 50% volume would be 82 cm^3 outside the center wires, or 90 cm^3 including inside the center wires.

Evaluation of Probes

The Hydra probe program estimated the real and imaginary components of permittivity. The other probes do not have a procedure for separating out the real component and are forced to rely on $\varepsilon_a^{1/2}$. Because the Hydra probe separated out the real component, site-specific calibrations for this probe should use the real component rather than $\varepsilon_a^{1/2}$. The Hydra probe program also gives output for temperature within probe head and for electrical conductivity. The electrical conductivity is calculated assuming the imaginary permittivity component is only due to electrical conductivity, which ignores the bound water relaxation component (Kelleners et al., 2005a; Logsdon, 2005a) given in Equation 7. The Hydra probe had larger RMSE (Table 1) than the ML2X and CS616, perhaps because of the lower measurement frequency. The lower measurement frequency was more sensitive to electrical conductivity influences, which increased at low frequencies (Equation 7), and were very temperature-sensitive.

Both the Hydra and ML2X probes have a multi-wire quasi-coaxial configuration. This configuration tends to concentrate the energy field around the center wire (Robinson et al., 2003), and could make the probes more sensitive to air gaps and minor soil variations than the parallel waveguide orientation of the CS616. The expense of the ML2X probes works against selecting them for automated field monitoring at several sites and depths.

The low cost of the CS616 and larger sample volume favored this probe for horizontal field installation and automated monitoring. At deeper depths, the installation of the CS616 could be more disruptive because the probe is longer, which increases the chance of encountering rocks. A dummy probe and insertion template would be suggestion for preliminary installation, even though this might create an air gap. The air gap would be worse if an unexpected rock were encountered, and waveguides were deflected.

For soils high in smectites, site-specific calibrations are recommended, no matter which soil moisture sensor is selected. Additional soil temperature data would be prudent since the temperature-corrected calibrations produced more realistic diurnal patterns of soil water content. Use of thermocouples in the field along with periodic soil moisture measurements (gravimetric or neutron probe for deeper depths) would be useful for on-site field calibration of these sensors.

References

[1] Allmaras, R.R., Nelson, W.W., & Voorhees, W.B. (1975). "Soybean and corn rooting in southwestern Minnesota: I. Water-uptake sink," *Soil Science Society of America Journal*, Vol. 39, No. 4, pp. 764-771.

[2] Anderson, M.G., & Burt, T.P. (1990). "Subsurface runoff." In (Anderson, M.G. and .P. Burt, Eds.) *Process Studies in Hillslope Hydrology*. John Wiley and Sons, New York. pp.367-400.

[3] Delta-T Devices. ThetaProbe Soil Moisture Sensor Type ML2X User Manual ML2X-Um-1.21. 22 pp. Delta-T Devices Ltd. Cambridge, England. 1999.

[4] Jackson, C.R. (1992). "Hillslope infiltration and lateral downslope unsaturated flow," *Water Resources Research*, Vol. 28, No. 9, pp. 2533-2539.

[5] Heimovaara, T.J., de Winter, E.J.G., van Loon, W.K.P., & Esveld, D.C. (1996). "Frequency-dependent dielectric permittivity from 0 to 1 GHz: Time domain reflectometry measurements compared with frequency domain network analyzer measurements," *Water Resources Research*, Vol. 32, No.12, pp. 3603-3610.

[6] Kelleners, T.J., Robinson, D.A., Shouse, P.J., Ayars, J.E., & Skaggs, T.H. (2005a). "Frequency dependence of the complex permittivity and its impact on dielectric sensor calibration in soils," *Soil Science Society of America Journal*, Vol. 69, No. 1, pp. 67-76.

[7] Kelleners, T.J., Seyfried, M.S., Blonquist, Jr., J.M., Bilskie, J., & Chandler, D.G. (2005b). "Improved interpretation of water reflectometer measurements in soils," *Soil Science Society of America Journal*, Vol. 69, No. 6, pp. 1684-1690.

[8] Knight, J.H. (1992). "Sensitivity of time domain reflectometry measurements to lateral variations in soil water content," *Water Resources Research*, Vol. 28, No. 9, pp. 2345-2352.

[9] Logsdon, S.D. (2000). "Effect of cable length on TDR calibration for high surface area soils," *Soil Science Society of America Journal*, Vol. 64, No. 1, pp. 54-61.

[10] Logsdon, S.D. (2005a). "Soil dielectric spectra from vector network analyzer data," *Soil Science Society of America Journal*, Vol. 69, No. 4, pp. 983-989.

[11] Logsdon, S.D. (2005b). "Time domain reflectometry range of accuracy for high surface area soils," *Vadose Zone Journal*, Vol. 4, No. 4, pp. 1011-1019.

[12] Logsdon, S.D. (2006). "Experimental limitations of time domain reflectometry hardware," *Soil Science Society of America Journal*, Vol. 70, No. 2, pp. 537-540.

[13] Maraux, F., & Lafolie, F. (1998). "Modeling soil water balance of a maize-sorghum sequence," *Soil Science Society of America Journal*, Vol. 62, No. 1, pp. 75-82.

[14] Morgan, C.P., & Stolt, M.H. (2004). "A comparison of several approaches to monitor water-table fluctuations," *Soil Science Society of America Journal*, Vol. 68, No. 2, pp. 562-566.

[15] Nachabe, M., Shah, N., Ross, M., & Vomacka, J. (2005). "Evapotranspiration of two vegetation covers in a shallow water table environment," *Soil Science Society of America Journal*, Vol. 69, No. 2, pp. 492-499.

[16] Philip, J. R. (1991). "Hillslope infiltration: planar slopes," *Water Resources Research*, Vol. 27, No. 1, pp. 109-117.

[17] Shang, J.Q., Rowe, R.K., Umana, J.A., & Scholte, J.W. (1999). "A complex permittivity measurement system for undisturbed / compacted soils." *Geotechnical Testing Journal* Vol. 22, No. 2, pp. 159-168.

[18] Stevens-Vitel. Hydra Soil Moisture Probe User's Manual Version 1.2 PN 92915 Rev.A. 22 pp. Stevens Vitel, Inc. Cantilly, Va. 1994.

[19] Van Bavel, C.H.M., & Ahmed, J. (1976). "Dynamic simulation of water depletion in the root zone," *Ecological Modeling*, Vol. 2, No. 3, pp. 189-212.

[20] Van Bavel, C.H.M., Brust, K.J., & Stirk, G.B. (1968). "Hydraulic properties of a clay loam soil and the field measurement of water uptake by roots. II. The water balance of the root zone," *Soil Science Society of America Proceedings*, Vol. 32, No. 2, pp. 317-321.

Biographical Information

Sally Logsdon obtained her B.A. degree in Biology with a Chemistry minor at Cedarville College, Cedarville, Ohio, her M.S. degree in soil physics at Michigan State University in East Lansing, Michigan, and her Ph.D. degree in soil physics from Virginia Polytechnical Institute at Blacksburg, Virginia. After completing a post-doctorate with the USDA-Agricultural Research Service in St. Paul, Minnesota, she obtained a soil scientist position with USDA-ARS at the National Soil Tilth Laboratory in Ames, Iowa, where she has worked for 16 years.

Brian Hornbuckle is currently an Assistant Professor in the Department of Agronomy (Crop, Soil, and Environmental Sciences) and the Department of Electrical and Computer Engineering at Iowa State University of Science and Technology in Ames. Dr. Hornbuckle graduated from Brown University in 1994 with a Sc.B. in electrical engineering. In 1996 he completed the M.A. in secondary education (science) at The University of Mississippi, Oxford. He received the M.S.E. in electrical engineering (electromagnetics) in 1997, and the Ph.D. in electrical engineering and atmospheric, oceanic, and space sciences (geoscience and remote sensing) in 2003, both from The University of Michigan, Ann Arbor.